—Original—

Exosome-Derived *microRNA-22* Ameliorates Pulmonary Fibrosis by Regulating Fibroblast-to-Myofibroblast Differentiation *in Vitro* and *in Vivo*

Naoyuki Kuse, Koichiro Kamio, Arata Azuma, Kuniko Matsuda, Minoru Inomata, Jiro Usuki, Akemi Morinaga, Toru Tanaka, Takeru Kashiwada, Kenichiro Atsumi, Hiroki Hayashi, Yoshinobu Saito, Masahiro Seike and Akihiko Gemma

Department of Pulmonary Medicine and Oncology, Graduate School of Medicine, Nippon Medical School, Tokyo, Japan

Background: Although aberrant proliferation and activation of lung fibroblasts are implicated in the initiation and progression of idiopathic pulmonary fibrosis (IPF), the underlying mechanisms are not well characterized. Numerous microRNAs (miRNAs) have been implicated in this process; however, miRNAs derived from exosomes and the relevance of such miRNAs to fibroblast-to-myofibroblast differentiation are not well understood. In this study, we attempted to identify exosome-derived miRNAs relevant to fibrosis development.

Methods: Using miRNA array analysis, we profiled exosome-derived miRNA expression in sera of C57BL/6 mice exhibiting bleomycin-induced pulmonary fibrosis. After validating a selected miRNA by quantitative reverse-transcription polymerase chain reaction, its effect on fibroblast-to-myofibroblast differentiation was investigated in human lung fibroblasts. Furthermore, we determined the role of the selected miRNA in an *in vivo* model of pulmonary fibrosis.

Results: MiRNA array analysis revealed that *miR-22* expression was increased by up to 2 fold on day 7 after bleomycin treatment compared with that in vehicle-treated mice. *In vitro*, *miR-22* transfection suppressed TGF-β1-induced α-SMA expression. This was mediated via inhibition of the ERK1/2 pathway. Baseline α-SMA expression was increased upon *miR-22* inhibitor transfection. Furthermore, *miR-22* negatively regulated connective tissue growth factor expression in the presence of TGF-β1. *In vivo*, administration of a *miR-22* mimic on day 10 after bleomycin challenge ameliorated pulmonary fibrosis lesions accompanied by decreased α-SMA expression in the model mice.

Conclusions: Exosomal *miR-22* modulates fibroblast-to-myofibroblast differentiation. The present findings warrant further study, which could shed light on *miR-22* as a novel therapeutic target in IPF.

(J Nippon Med Sch 2020; 87: 118–128)

Key words: idiopathic pulmonary fibrosis, exosome, microRNA, myofibroblast differentiation

Introduction

Idiopathic pulmonary fibrosis (IPF) is a progressive and devastating lung disorder with a poor prognosis[1].

The pathogenesis of IPF is not fully understood; however, formation of fibroblastic foci and excessive deposition of extracellular matrix proteins are regarded as factors that directly cause IPF[2]. Although disease progression is variable and unpredictable, median survival time from diagnosis is estimated to be 2 to 4 years[3,4]. Because available therapeutics are limited[5,6], novel therapeutic strategies are urgently needed.

MicroRNAs (miRNAs) are small, non-coding, single-stranded RNA molecules that mediate mRNA cleavage, translational repression, and mRNA destabilization[7]. Emerging evidence indicates that miRNAs are involved in the development of organ fibrosis[8]. In patients with IPF, accumulating data suggest significant changes in the expression of miRNAs, including *miR-21*[9,10], *Let-7d*[11], and

Correspondence to Koichiro Kamio, Department of Pulmonary Medicine and Oncology, Graduate School of Medicine, Nippon Medical School, 1–1–5 Sendagi, Bunkyo-ku, Tokyo 113–8603, Japan
E-mail: bcway@nms.ac.jp
https://doi.org/10.1272/jnms.JNMS.2020_87-302
Journal Website (https://www.nms.ac.jp/sh/jnms/)

miR-200[12]. Recently, Liu et al.[13] reported that decreased expression of *miR-30a* might be associated with IPF progression. Moreover, Ren et al.[14] indicated that *miR-541* might play a key role in the formation of lung fibrosis. MiRNAs are encapsulated in exosomes, which are 40- to 100-nm vesicles that are released from several cell types participating in intercellular communication[15].

Although multiple classes of cells are involved in the pathogenesis of IPF, lung fibroblast-to-myofibroblast differentiation is a key event in IPF initiation and progression[16,17].

Among numerous growth factors, the transforming growth factor-β1 (TGF-β1) signaling pathway is the main cascade implicated in myofibroblast differentiation[18]. After binding to its receptor, TGF-β1 induces numerous events, including extracellular matrix production and α-smooth muscle actin (α-SMA) expression, which are signaled in a Smad-dependent or -independent manner. Kang recently reported several miRNAs involved in TGF-β signaling-mediated lung fibrosis[19], and *miR-101*[20], *miR-9-5p*[21], *miR-1343*[22], and *miR-27b*[23] were found to interfere with fibroblast-to-myofibroblast differentiation. Similarly, *miR-27a* repressed myofibroblast differentiation[16].

In this study, we aimed to identify exosome-derived miRNAs relevant to fibroblast-to-myofibroblast differentiation. To achieve this, we utilized a well-characterized bleomycin (BLM)-induced murine pulmonary fibrosis model. Exosome-derived miRNAs were subjected to miRNA array analysis to characterize time-dependent changes in miRNA expression within exosomes in serum.

Materials and Methods

Animals and BLM Treatment

In the present study, we used 12-week-old male SPF C57BL/6 mice (Charles River Laboratories Japan, Yokohama, Japan). Osmotic pumps (ALZET, model 2001; Durect Corporation, Cupertino, CA, USA) containing 200 μL of saline with or without BLM (100 mg/kg body weight; Nippon Kayaku Co., Tokyo, Japan) were implanted subcutaneously through a small incision in the back, in accordance with the manufacturer's instructions, on day 0 (**Fig. 1A**)[24,25]. Incision wounds were sealed with a surgical suture. BLM was continuously infused via the pumps for 7 days, in accordance with the manufacturer's instructions. The experimental protocols were approved (approval number, 29-056) by the Animal Care and Use Committee of the Nippon Medical School, Tokyo, Japan.

Exosome Extraction and miRNA Array Analysis

Exosomes were extracted with ExoQuick (System Biosciences, LLC, Palo Alto, CA, USA) from mouse sera on day 0 before BLM challenge, and on days 7, 14, 21, and 28 after BLM challenge (**Fig. 1A**). Briefly, ExoQuick Exosome Precipitation Solution was added to the serum, which was then refrigerated in accordance with the manufacturer's protocol. The ExoQuick/biofluid mixture was centrifuged at 1,500 × *g* at 4°C for 30 min. After centrifugation, the exosomes appeared as a beige or white pellet and were resuspended in sterile water. Exosome presence and purity were confirmed by western blot analysis (see below) of the lysates by using anti-CD63, CD81, and TSG101 antibodies (Santa Cruz Biotechnology, Inc., Dallas, TX, USA). MiRNAs within exosomes were extracted with a mirVana miRNA Isolation Kit (Life Technologies, Carlsbad, CA, USA) and analyzed with the 3D-GENE miRNA oligo chip (Toray Industries Inc., Tokyo, Japan), in accordance with the manufacturer's protocol.

Quantitative Reverse-Transcription (qRT)-PCR Analysis of miRNA Expression

The isolated miRNAs were converted to complementary DNA. Expression of *miR-22* and *snoRNA423* (a constitutively expressed "housekeeping" gene used as a control) was quantified by qRT-PCR using the TaqMan Gene Expression Assay Kit (Applied Biosystems Japan, Ltd., Tokyo, Japan), the Thunderbird Probe qPCR Mix (Toyobo, Osaka, Japan), and the 7500 Fast Real-Time PCR System (Applied Biosystems). *MiR-22* expression was normalized to that of *snoRNA423*.

Cell Culture

Human fetal lung fibroblast (HFL-1) cells (RCB0521, Riken BRC Cell Bank, Ibaraki, Japan) were maintained in 75-cm^2 Nunc EasyFlask cell-culture flasks (Thermo Fisher Scientific Inc., Waltham, MA, USA) containing Roswell Park Memorial Institute (RPMI)-1640 medium supplemented with 10% fetal calf serum, 100 μg/mL penicillin, and 250 μg/mL streptomycin sulfate (Fujifilm Wako Pure Chemical Corporation, Osaka, Japan) at 37°C, with 5% CO_2, in a humidified atmosphere. Subconfluent cells (passage 14-18) were treated with *miR-22* mimic, *miR-22* inhibitor (see below), and/or TGF-β1 (5 ng/mL; R&D Systems Inc., Minneapolis, MN, USA).

MiRNA Mimic or Inhibitor Transfection

MiR-22 mimic, *miR-22* inhibitor, or a negative control oligonucleotide consisting of a random sequence of bases (Ambion, Foster City, CA, USA) was transiently transfected into HFL-1 cells by using Lipofectamine iMAX (Invitrogen, Carlsbad, CA, USA), in accordance with the manufacturer's instructions.

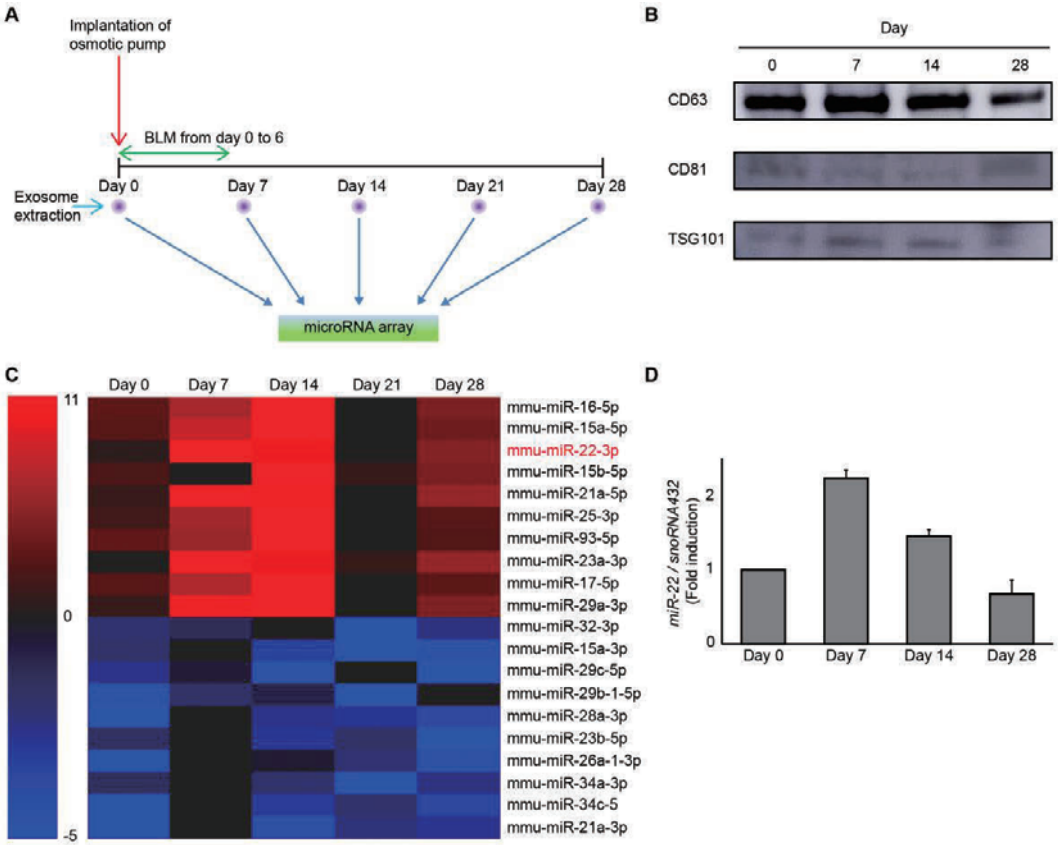

Fig. 1 Identification of important exosome-derived microRNAs (miRNAs) that might be involved in bleomycin (BLM)-induced murine pulmonary fibrosis. (**A**) Outline of experimental design used for selection of miRNA candidates by using a comprehensive miRNA array-based approach. Osmotic pumps containing 200 μL of saline, with or without BLM (100 mg/kg mouse body weight), were implanted subcutaneously through a small incision in the back, according to the manufacturer's instructions. BLM was infused continuously from days 0 to 6. Exosomes were extracted by using ExoQuick™ from sera of mice collected on day 0 before BLM challenge and on days 7, 14, 21, and 28 post BLM challenge. MiRNAs extracted from the exosomes were then hybridized to the Toray 3D-Gene® miRNA array (n = 2-3 mice per time point). (**B**) Lysates prepared from the extracted exosomes were subjected to western blot analysis to confirm the presence of exosomes, using anti-CD63, CD81, and TSG101 antibodies. (**C**) Heat maps displaying differential expression of miRNAs at the indicated time points after BLM challenge. The 10 most strongly upregulated (red) and downregulated (blue) 2-digit miRNAs were selected for further analysis. (**D**) Validation of exosome-derived *miR-22* expression. MiRNAs were extracted from exosomes and converted to cDNA. Relative expressions of *miR-22* and *snoRNA432* were quantified by quantitative reverse-transcription PCR. The relative expression of *miR-22* was normalized against that of *snoRNA432*, and fold-change relative to that of a saline-treated group is presented. Results from two independent experiments assayed in duplicate are presented. The relative expression of exosome-derived *miR-22* in BLM-treated mice was upregulated by up to 2-fold on day 7, as compared with that in the control mice.

Western Blot Analysis

Cells from subconfluent cultures were washed twice with PBS, scraped into PBS, and pelleted via centrifugation. Whole-cell lysates were prepared in Radio-Immunoprecipitation Assay (RIPA) buffer (Fujifilm Wako Pure Chemical Corporation) for immunoblotting. Protein concentrations were determined by using the BCA Protein Assay Kit (Thermo Fisher Scientific Inc.), according to the manufacturer's instructions, with bovine serum albumin as the standard. Samples were resolved via sodium dodecyl sulfate-polyacrylamide gel electrophoresis under reducing conditions and transferred onto polyvinylidene difluoride membranes (Bio-Rad Laboratories, Hercules, CA, USA). The membranes were blocked with 5% skim milk in Tris-buffered saline (0.15 M NaCl and 0.05 M Tris-HCl [pH 8.0], and 0.05% [v/v] Tween 20) and

incubated with primary antibodies at the manufacturer's recommended dilutions. Primary antibodies against extracellular signal-regulated protein kinase (ERK)1/2, phospho (p-)ERK1/2, (p-)Smad2, (p-)Smad3, and TGFβRI were purchased from Cell Signaling Technology, Inc. (Danvers, MA, USA). A mouse monoclonal anti-α-SMA antibody was purchased from Dako (Glostrup, Denmark). A mouse monoclonal anti-β-actin antibody (clone AC-74) purchased from Sigma-Aldrich Corporation (St. Louis, MO, USA) and anti-glyceraldehyde-3-phosphate dehydrogenase (GAPDH) antibody purchased from Santa Cruz Biotechnology, Inc. (Dallas, TX, USA) were used as the loading and transfer controls. After incubation with either anti-mouse IgG2b HRP-conjugated secondary antibody (SouthernBiotech, Birmingham, AL, USA) or anti-rabbit IgG HRP-conjugated secondary antibody (SouthernBiotech), protein bands were detected with the ImmunoStar LD system (Fujifilm Wako Pure Chemical Corporation), in accordance with the manufacturer's instructions, and were photographed with an Amersham Imager 600 (GE Healthcare Life Sciences, Marlborough, MA, USA). The bound antibodies were then removed by incubating the membranes in Restore Western Blot Stripping Solution (Fujifilm Wako Pure Chemical Corporation), in accordance with the manufacturer's protocol, and then reprobed. Protein band intensity was quantified via densitometry by using ImageJ 1.48 software (National Institutes of Health, Bethesda, MD, USA).

Immunocytochemistry

Changes in α-SMA protein expression were visualized by immunofluorescence, as previously described[26]. Briefly, HFL-1 cells were seeded in a 12-well plate (Thermo Fisher Scientific Inc.) and, after 48 h of transfection with *miR-22* mimic (50 nM), the cells were treated with TGF-β1 (5 ng/mL) for another 72 h. The cells were then washed with PBS and fixed in 4% paraformaldehyde at room temperature for 30 min. Subsequently, the cells were blocked with 3% goat serum at room temperature for 30 min and incubated for 10 min with PBS containing 0.1% TritonX-100 (Sigma-Aldrich Japan, Tokyo, Japan) before stained with anti-human α-SMA antibody (Dako) at 4°C overnight. Thereafter, the cells were incubated with secondary biotin-conjugated anti-rabbit IgG antibody at room temperature for 1 h and stained with Alexa Fluor 488-conjugated streptavidin (Life Technologies Corporation, CA, USA) at room temperature for 1 h. Nuclei were counterstained with 4' , 6-diamidino-2-phenylindole (DAPI). Finally, the sections were observed with a fluorescence microscope BZ-X800 (Keyence, Osaka, Japan).

Small Interfering RNA (siRNA) Transfection

SiRNA targeting connective tissue growth factor (CTGF) and non-targeting control (which were synthesized by Thermo Fisher Scientific) were transfected into cells at a final concentration of 50 nM with Lipofectamine RNAiMAX (Thermo Fisher Scientific) at 48 h after cell seeding, in accordance with the manufacturer's instructions. Then, cells were incubated at 37°C for 48 h.

RNA Extraction from Lung Fibroblasts and qRT-PCR

Total RNA was extracted from cultured HFL-1 cells by using ISOGEN reagents with spin columns (Nippon Gene, Tokyo, Japan) and converted to complementary DNA. *CTGF* and *GAPDH* mRNA expression was measured by qRT-PCR using the TaqMan Gene Expression Assay (Applied Biosystems Japan, Ltd.) and Thunderbird Probe qPCR Mix on an Applied Biosystems 7500 Fast Real-Time PCR System. The relative amounts of *CTGF* mRNA were normalized to *GAPDH* mRNA expression levels.

Administration of a *miR-22* Mimic to Mice Exhibiting BLM-Induced Pulmonary Fibrosis

A *miR-22* mimic or scrambled RNA (1 nmol/mouse) (GeneDesign Inc., Osaka, Japan) was administered intravenously via the tail vein on day 10 after BLM challenge. Mice were sacrificed on day 28, and the lungs were removed and subjected to histological and biochemical analyses.

Histological Examination of Pulmonary Tissues

Lung samples were fixed in 10% formalin buffer (Fujifilm Wako Pure Chemical Corporation) and embedded in paraffin. Paraffin sections (thickness, 3 μm) were cut and stained with hematoxylin-eosin and Masson's trichrome stain to assess gross morphology and collagen deposition, respectively, and examined by microscopy. Lung fibrosis was measured by quantitative histology using Ashcroft's method[27].

Evaluation of Lung Fibrosis with Collagen Measurement

Total lung collagen was determined by using a Sircol Collagen Assay kit (Biocolor Ltd., Carrickfergus, Northern Ireland, UK), in accordance with the manufacturer's instructions. Briefly, lungs were harvested on day 28 and homogenized in 0.5 M acetic acid (50 volumes to wet lung weight) containing approximately 1 mg pepsin/10 mg tissue residue. Each sample was incubated for 24 h at room temperature with stirring. After centrifugation, 100 μL of each supernatant was assayed. One milliliter of Sircol dye reagent, which binds to collagen, was added to each sample and mixed for 30 min. After centrifugation,

the pellets were suspended in 1 mL of the alkali reagent included in the kit and read at 540 nm with a spectrophotometer. Collagen standard solutions were used to construct a standard curve. Collagens contain approximately 14% hydroxyproline by weight, and the collagen values obtained with this method correlated well with the hydroxyproline content reported in the manufacturer's data.

Immunohistochemistry for α-SMA

Sections of paraffin-embedded lung lobes were deparaffinized and rehydrated. Antigen retrieval was achieved by boiling at 105°C for 7 min in 10 mM citrate buffer (pH 6.0), followed by gradual cooling to room temperature. Then, the sections were treated with 3% hydrogen peroxide in methanol for 20 min and blocked with 10% normal goat serum (Nichirei Biosciences, Inc., Tokyo, Japan) at room temperature for 20 min. Sections were incubated with an anti-α-SMA antibody (Abcam, Cambridge, MA, USA) for 1 h at room temperature. For α-SMA staining, tissue sections were incubated with a secondary anti-rabbit antibody, Histofine Simple Stain Mouse MAX-PO (R) (Nichirei Biosciences, Inc.), for 30 min at room temperature. Then, an ImmPACT DAB Peroxidase Substrate Kit (Vector, Burlingame, CA, USA) was used to visualize α-SMA expression and counterstained with hematoxylin.

Statistical Analysis

Comparisons between multiple groups were made by using one-way analysis of variance; Tukey-Kramer *post-hoc* correction was used to adjust for multiple comparisons. The unpaired two-tailed Student's *t*-test was used for all single comparisons. The data were analyzed with JMP 9 software, version 9.0.3 (SAS Institute Inc., Cary, NC, USA), and are expressed as mean ± SD. A P value of <0.05 was considered to indicate statistical significance.

Results

Tentative Upregulation of Exosomal *miR-22* in Sera from Mice with BLM-Induced Pulmonary Fibrosis

As an initial assessment, we screened for exosome-derived miRNAs implicated in lung fibrosis by observing time-dependent changes in exosomal miRNAs during the course of BLM-induced murine pulmonary fibrosis. To this end, we first isolated exosomes from sera of mice with BLM-induced pulmonary fibrosis (**Fig. 1A**). Exosomes were characterized at the protein level by the presence of CD63, CD81, and TSG101 (**Fig. 1B**). Then, we extracted miRNAs from the exosomes and hybridized them to a miRNA array containing 1,900 miRNAs. As shown in **Figure 1C**, we successfully identified ten 2-digit miRNAs that exhibited the highest degree of up- or downregulation. In this panel, *miR-22* was the third most strongly upregulated miRNA after BLM challenge; however, its effect on myofibroblast differentiation in the lungs has not been determined. Therefore, we focused on this miRNA in subsequent analyses. Validation analysis of *miR-22* expression by qRT-PCR revealed that its expression in exosomes derived from BLM-treated mouse sera was upregulated by up to 2-fold on day 7, as compared with that of control mice, and declined thereafter (**Fig. 1D**).

MiR-22* Mimic Suppresses TGF-β1-Induced α-SMA Expression in Human Lung Fibroblasts *in Vitro

Fibroblast-to-myofibroblast differentiation is induced upon TGF-β1 treatment and is characterized by α-SMA expression[18,19]. The inhibitory effect of *miR-22* on myofibroblast differentiation was demonstrated in studies using cardiac fibroblasts isolated from rats[28]; however, the effect of *miR-22* has not been determined in human lung fibroblasts. Therefore, we transfected HFL-1 cells with *miR-22* mimic before the addition of TGF-β1 and then evaluated α-SMA expression by western blot analysis. As shown in **Figure 2A**, TGF-β1-induced α-SMA expression was significantly attenuated by the *miR-22* mimic. To confirm this result, we performed immunofluorescence staining of α-SMA. As shown in **Figure 2B**, TGF-β1-induced cytosolic α-SMA expression (green) was ameliorated by *miR-22* transfection. Next, we evaluated whether *miR-22* inhibitor would affect α-SMA expression. As shown in **Figure 2C**, *miR-22* inhibitor slightly enhanced α-SMA expression under normal physiological conditions.

***MiR-22* Modulates the ERK Signaling Pathway in Human Lung Fibroblasts**

Hong et al.[28] demonstrated that *miR-22* affects TGF-β1 signaling by interfering with TGFβRI expression. Therefore, we examined whether *miR-22* inhibits TGFβRI expression in human lung fibroblasts. However, *miR-22* had no effect on TGFβRI expression (data not shown). Fierro-Fernandez et al.[21] reported that miR-9-5p inhibits TGF-β1 signaling by regulating Smad2 phosphorylation; thus, we next assessed whether *miR-22* inhibited Smad signaling. Again, the results indicated this was not the case (data not shown). Midgley et al.[29] reported that TGF-β1-induced myofibroblast differentiation is mediated via ERK1/2; therefore, we examined whether this pathway is a target of *miR-22*. As shown in **Figure 3**, western blot analysis revealed that *miR-22* decreased TGF-β1-induced ERK1/2 phosphorylation at the indicated time points.

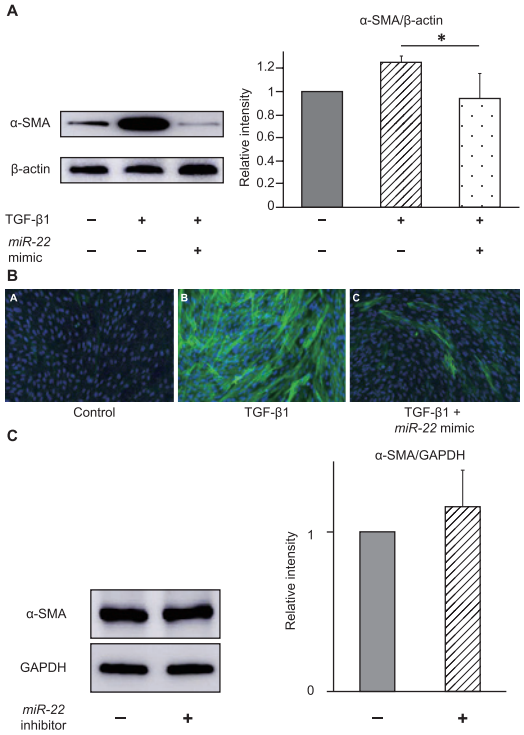

Fig. 2 Effect of *miR-22* mimic on TGF-β1-induced α-smooth muscle actin (α-SMA) expression in human lung fibroblasts. (**A**) Monolayer-cultured human fetal lung fibroblasts (HFL-1 cells) were serum-starved for 24 h before transfection of a *miR-22* mimic (50 nM). The cells were cultured for 48 h with a *miR-22* mimic before the addition of TGF-β1 (5 ng/mL) and further cultured for 72 h. Whole-cell lysates were prepared and subjected to western blot analysis by using an antibody against α-SMA. A representative blot from three independent experiments is presented (left). α-SMA signal intensity was normalized to that of β-actin and expressed relative to that in cells treated with scrambled miRNA (right). ImageJ software was used for signal quantification. The *miR-22* mimic significantly reversed TGF-β1-induced α-SMA expression (*$P < 0.05$ by Student's *t*-test). (**B**) HFL-1 cells were grown in a 12-well plate and transfected with *miR-22* mimic (50 nM) for 48 h before incubation with TGF-β1 (5 ng/mL) for another 72 h. HFL-1 cells were stained with an anti-α-SMA antibody. Nuclei were counterstained with DAPI. Original magnification, 200×. (**C**) HFL-1 cells were cultured with a *miR-22* inhibitor (50 nM) for 72 h. Whole-cell lysates were prepared and subjected to western blot analysis by using an antibody against α-SMA. A representative blot from two independent experiments is presented (left). α-SMA signal intensity was normalized to that of GAPDH and expressed relative to that in cells treated with scrambled miRNA (right). ImageJ software was used for signal quantification. The *miR-22* inhibitor slightly stimulated α-SMA expression under normal physiological conditions.

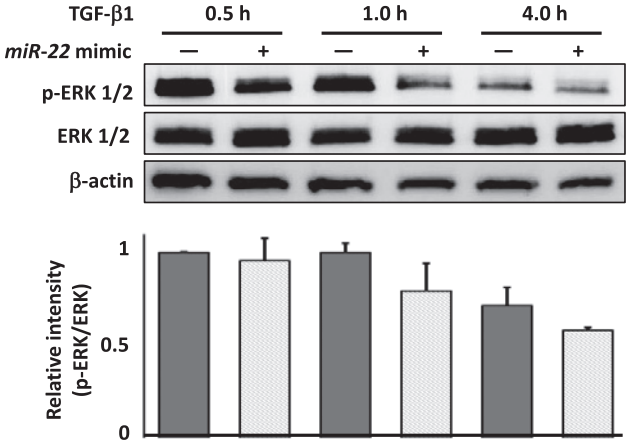

Fig. 3 *MiR-22* mimic modulates TGF-β1-induced extracellular signal-regulated kinase (ERK) 1/2 signaling. Monolayer-cultured human fetal lung fibroblasts (HFL-1 cells) were serum-starved for 24 h before transfection of a *miR-22* mimic (50 nM). The cells were cultured for 48 h with the *miR-22* mimic before the addition of TGF-β1 (5 ng/mL). Cells were harvested at 0.5, 1.0, and 4.0 h after the addition of TGF-β1, and whole-cell lysates were subjected to western blot analysis by using antibodies against ERK and phospho (p) -ERK. A representative blot from two independent experiments is presented in the upper panel. Relative intensity analysis of each band was conducted with ImageJ software. Fold changes in p-ERK/ERK expression are presented in the lower panel. The *miR-22* mimic decreased TGF-β1-induced p-ERK at each time point.

A *miR-22* Mimic Modulates Myofibroblast Differentiation via Regulation of CTGF

CTGF is known to upregulate α-SMA expression in human lung fibroblasts[30]. In support of this finding, we observed that siCTGF attenuated baseline and TGF-β1-induced α-SMA expression (**Fig. 4A**). To assess whether *miR-22* affects CTGF expression, we transfected HFL-1 cells with a *miR-22* mimic and investigated changes in TGF-β1-induced *CTGF* mRNA expression. As shown in **Figure 4B**, the *miR-22* mimic inhibited *CTGF* mRNA expression in the presence of TGF-β1.

Effect of a *miR-22* Mimic on BLM-Induced Murine Pulmonary Fibrosis

The above results prompted us to hypothesize that inhibiting fibroblast differentiation by replenishing *miR-22* would prevent development of pulmonary fibrosis. To test this, we intravenously administered a *miR-22* mimic to mice with BLM-induced pulmonary fibrosis via the tail vein on day 10 after BLM challenge. On day 28, the mice were sacrificed, and the lungs were removed and

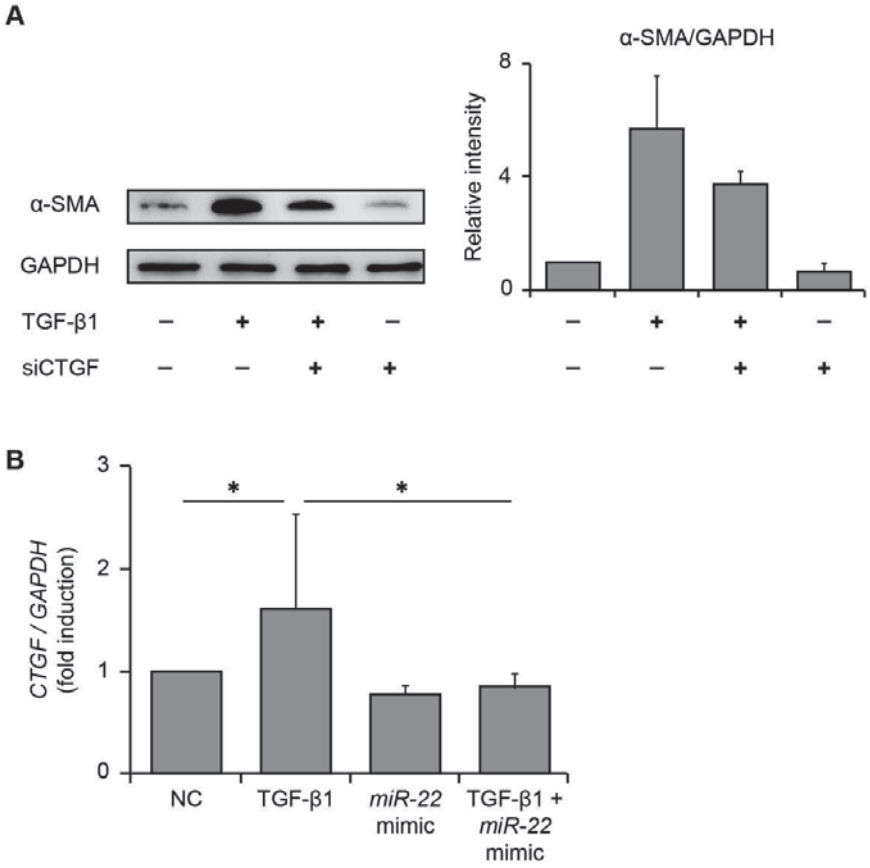

Fig. 4 Connective tissue growth factor (CTGF) is regulated by *miR-22* in response to TGF-β1. (**A**) Monolayer-cultured human fetal lung fibroblasts (HFL-1 cells) were serum-starved for 24 h before transfection of small interfering (si)CTGF (50 nM). The cells were cultured for 48 h with siCTGF before the addition of TGF-β1 (5 ng/mL) and were then cultured for another 72 h. Whole-cell lysates were prepared and subjected to western blot analysis by using an antibody against α-SMA. A representative blot from three independent experiments is presented (left). α-SMA signal intensity was normalized to that of GAPDH and expressed relative to that in cells treated with scrambled siRNA (right). ImageJ software was used for signal quantification. siCTGF attenuated α-SMA expression under both normal physiological (lane 4) and TGF-β1-stimulated (lane 3) conditions. (**B**) HFL-1 cells cultured in monolayers were serum-starved for 24 h before being treated with the *miR-22* mimic (50 nM) for 48 h. Then, the cells were treated with TGF-β1 (5 ng/mL) for another 48 h. Total cellular RNA was harvested to analyze *CTGF* mRNA expression by qRT-PCR. The *miR-22* mimic inhibited *CTGF* mRNA expression in the presence of TGF-β1.

subjected to immunohistochemical and biochemical analyses (**Fig. 5A**). Lung histological data revealed focal fibroplasias with destruction of the alveolar wall in the group receiving BLM (**Fig. 5B and C**). Injection of the *miR-22* mimic on day 10 ameliorated the lesions (**Fig. 5D and E**). To quantify the antifibrotic effects of *miR-22* in the lungs of BLM-treated mice, we determined the extent of lung fibrosis by quantitative histology, according to Ashcroft's method, on day 28 after treatment. Because BLM administration via osmotic pumps causes lung fibrosis predominantly in the subpleural regions[31,32], subpleural fibrosis between the groups was compared by using a numerical scale. Two blinded observers (NK and MI) quantified fibrosis in each section. Fibrosis scores were significantly lower in mice that had received the *miR-22* mimic on day 10 (**Fig. 5F**, $*P < 0.05$). As shown in **Figure 5G**, collagen content in the lungs was attenuated when the *miR-22* mimic was infused to BLM-treated mice. Using immunohistochemical staining, we further examined whether α-SMA expression in the lungs of

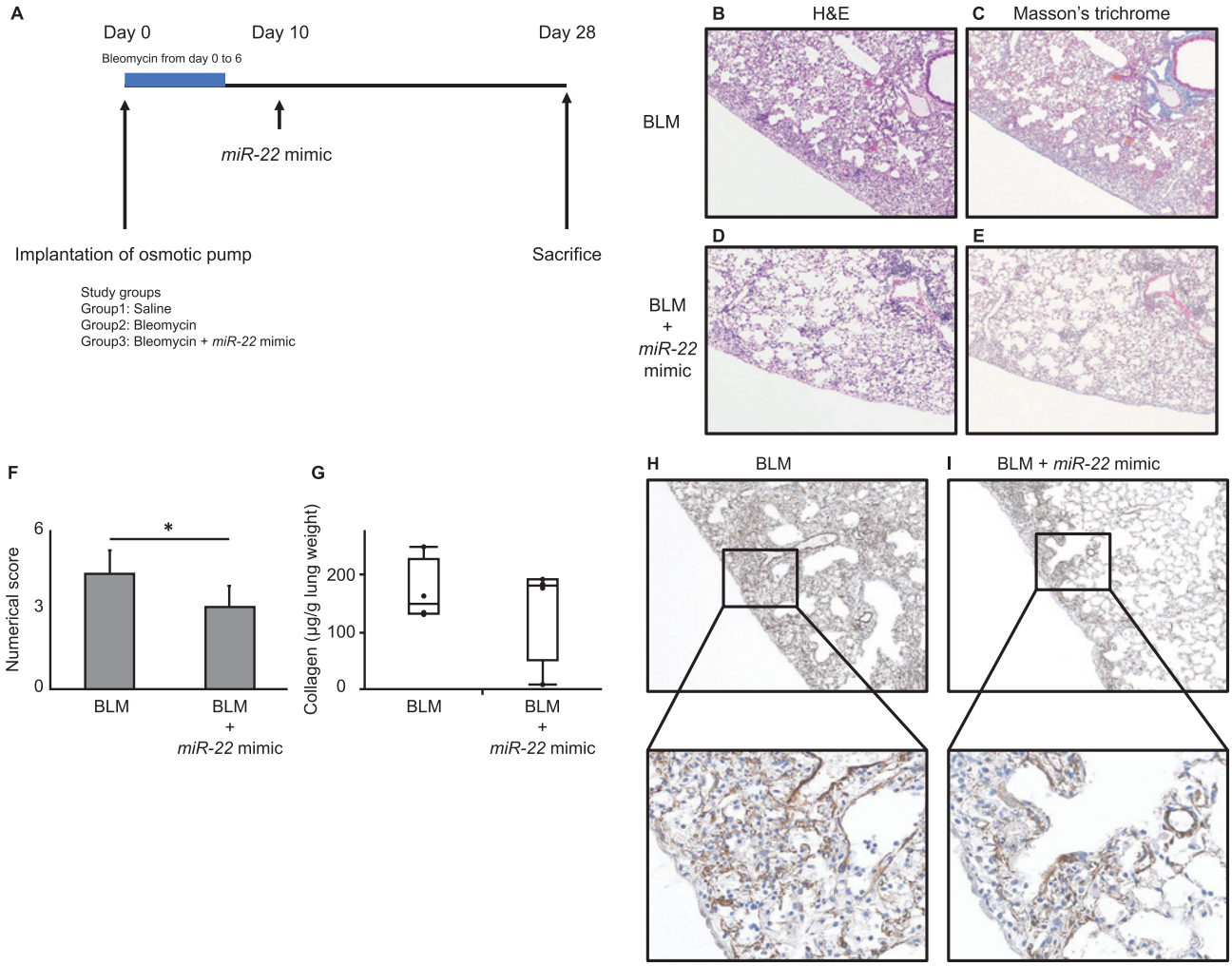

Fig. 5 *MiR-22* mimic suppresses bleomycin (BLM) -induced murine pulmonary fibrosis. (**A**) Outline of experimental design used for the administration of *miR-22* mimic. Animals were subcutaneously implanted with osmotic pumps that contained BLM (100 mg/kg body weight) or saline vehicle. BLM was infused continuously from day 0 to 6. The *miR-22* mimic (1 nmol/mouse) was injected intravenously via the tail vein on day 10 after initiating BLM treatment. On day 28 post BLM injection, the mice were sacrificed and their lungs were collected for analyses. (**B-E**) Increased fibrosis and collagen deposition observed in the lungs of BLM-treated mice were attenuated by injection of the *miR-22* mimic on day 10 after BLM treatment. Representative photomicrographs of H&E and Masson's trichrome staining of the left lungs from BLM-treated mice, with or without *miR-22* mimic injection (magnification, 40×). (**F**) The extent of lung fibrosis was measured by quantitative histology according to Ashcroft's method on day 28 to determine the antifibrotic effects of the *miR-22* mimic in the lungs of BLM-treated mice. Because BLM administration with osmotic pumps causes lung fibrosis predominantly in the subpleural regions, a numerical scale was used to compare subpleural fibrosis between groups. Administration of the *miR-22* mimic on day 10 significantly attenuated the increase in subpleural fibrosis score induced by BLM administration (*$P < 0.05$ by Student's *t*-test; n = 4 mice for BLM group, n = 6 mice for BLM + *miR-22* mimic group). (**G**) The amount of collagen was quantified to assess the antifibrotic effects of the *miR-22* mimic in the lungs of BLM-treated mice. Infusion of the *miR-22* mimic decreased collagen content in the lungs of BLM-treated mice (n = 4 mice for each group). (**H-I**) Immunohistochemical staining for α-SMA (brown) in lungs of mice with BLM-induced pulmonary fibrosis, without or with *miR-22* mimic injection (**H** and **I**, respectively). α-SMA-positive cells were markedly increased by BLM treatment (**H**), and this increase was attenuated by *miR-22* (**I**). Magnification = 4× and 20×.

BLM-treated mice was altered by *miR-22* mimic administration on day 10 after BLM challenge. Immunoreactivity for α-SMA was increased in fibrotic regions in BLM-treated mice (**Fig. 5H**), but this increase was attenuated upon *miR-22* injection, along with amelioration of fibrosis (**Fig. 5I**).

Discussion

In the present study, we observed a robust increase in the expression of exosomal *miR-22* in sera of mice with BLM-induced pulmonary fibrosis on day 7 post BLM challenge. *In vitro*, transfection of a *miR-22* mimic into human lung fibroblasts significantly inhibited TGF-β1-induced α-

SMA expression. Conversely, α-SMA protein expression was increased upon transfection of a *miR-22* inhibitor under normal physiological conditions. The effect of the *miR-22* mimic was proven to be mediated via TGF-β1-induced p-ERK1/2 inhibition. Furthermore, *miR-22* inhibited CTGF expression, which could lead to suppression of CTGF-induced α-SMA expression. *In vivo*, injection of the *miR-22* mimic into mice with BLM-induced pulmonary fibrosis ameliorated the lesions, thereby decreasing α-SMA expression in the lungs. These results delineate a novel regulatory mechanism involved in fibroblast-to-myofibroblast differentiation in response to miRNA.

Interestingly, although *miR-22* expression was upregulated in exosomes derived from mouse sera after BLM challenge in the present study, several studies have reported downregulation of miRNAs, including *miR-101*[20] and *miR-27b*[23], after BLM administration. Differences in study design could account for this inconsistency; we detected upregulation of *miR-22* expression in serum-derived exosomes, whereas *miR-101* and *miR-27b* were downregulated in lungs of BLM-treated mice. The precise origin of the exosomes detected in this study has yet to be defined; however, they are likely to have been secreted in tissues other than the lungs and to have been delivered to the lungs, the components of which are decreased as a result of BLM administration. Furthermore, the approach used to establish the BLM-induced pulmonary fibrosis model likely affected the results; we used osmotic pumps to induce pulmonary fibrosis because lung fibrosis is observed in the subpleural regions and the distribution of lesions is similar to that observed in human IPF, whereas Huang et al.[20] and Zeng et al.[23] used intranasal administration of BLM in their studies of *miR-101* and *miR-27b*, respectively. Use of the same model to investigate *miR-22* expression in the lungs could help clarify the roles of this miRNA and exosomes.

Exosomes are secreted by most cell types via exocytosis, containing and transferring various biomolecules, such as DNA, RNA, proteins, and lipids[33,34]. Studies on the relevance of exosomes in IPF pathogenesis have yielded contradictory results. Tan et al.[35] reported that exosomes derived from human amnion epithelial cells ameliorated experimental lung fibrosis, whereas Martin-Medina et al.[36] showed that WNT-5A-carrying exosomes derived from bronchoalveolar lavage fluid from experimental fibrotic lungs and patients with IPF accelerated disease progression. Thus, studies of the effects of *miR-22*-carrying exosomes on BLM-induced pulmonary fibrosis are warranted.

In this study, *miR-22* interfered with the ERK1/2 signaling pathway, resulting in amelioration of TGF-β1-induced α-SMA expression. However, Hong et al.[28] reported that *miR-22* inhibited myofibroblast differentiation by modulating TGFβRI expression in rat cardiac fibroblasts. The present study was designed to use fibroblasts from human lungs, while Hong et al. observed the effect of *miR-22* in cardiac fibroblasts from rats. Fibroblasts are heterogeneous, and the different sources of fibroblasts used in their and our studies might, in part, account for the discrepant results.

Our findings suggest that *CTGF* mRNA expression was attenuated by *miR-22*. CTGF plays an essential role in tissue repair and pulmonary fibrogenesis. Yang et al.[30] reported that CTGF stimulated lung fibroblast differentiation *in vitro* and *in vivo*. In a previous report, Yang et al.[37] reported that *miR-18a* regulated CTGF expression via the TGF-β1 signaling pathway in lung fibroblasts. Further, *miR-19a*, *19b*, and *26b* are reportedly involved in CTGF expression and pulmonary fibroblast differentiation[38]. However, the association between *miR-22* and CTGF expression was not previously described. Therefore, this study has revealed a novel CTGF regulatory mechanism.

The present miRNA array results show that *miR-16* was most strongly upregulated after BLM challenge. This miRNA targets the 3' untranslated region of the mTORC2 component-encoding gene *Rictor*[39]. Notably, we previously observed that *miR-16* inhibited BLM-induced murine pulmonary fibrosis by targeting the mTORC2-secreted protein acidic and rich in cysteine (SPARC) axis[40]. The second most strongly induced miRNA, *miR-15a*, was among the 161 miRNAs that were previously reported to be differentially expressed in the lungs of BLM-treated and control mice[8]. The present study was the first to assess the role of *miR-22* in the context of pulmonary fibrosis. Thereby, we focused on the function of *miR-22* throughout the study and found that this miRNA regulated myofibroblast differentiation.

In conclusion, we demonstrated that exosomal *miR-22* modulates fibroblast-to-myofibroblast differentiation. Future studies should investigate *miR-22* as a potential novel therapeutic target for IPF.

Acknowledgements: We thank Keyence Corporation for assistance with the experiments.

This work was supported by a Public Interest Trust Satoshi Okamoto Memorial Lung Fibrosis Research Fund (KK).

Grant-in-Aid for Scientific Research from the Ministry

of Education, Culture, Sports, Science and Technology of Japan.

Conflict of Interest: K. Kamio reports grants from Public Interest Trust Satoshi Okamoto Memorial Lung Fibrosis Research Fund, during the conduct of the study. A. Azuma and A. Gemma received personal fees from Nippon Kayaku Co., Tokyo, Japan. All other authors have nothing to disclose.

References

1. American Thoracic Society; European Respiratory Society. American Thoracic Society/European Respiratory Society International Multidisciplinary Consensus Classification of the Idiopathic Interstitial Pneumonias. This joint statement of the American Thoracic Society (ATS), and the European Respiratory Society (ERS) was adopted by the ATS board of directors, June 2001 and by the ERS Executive Committee, June 2001. Am J Respir Crit Care Med. 2002;165:277–304.
2. Selman M, Thannickal VJ, Pardo A, Zisman DA, Martinez FJ, Lynch JP 3rd. Idiopathic pulmonary fibrosis: pathogenesis and therapeutic approaches. Drugs. 2004;64:405–30.
3. Ley B, Collard HR, King TE Jr. Clinical course and prediction of survival in idiopathic pulmonary fibrosis. Am J Respir Crit Care Med. 2011;183:431–40.
4. Richeldi L, Collard HR, Jones MG. Idiopathic pulmonary fibrosis. Lancet. 2017;389:1941–52.
5. King TE Jr, Bradford WZ, Castro-Bernardini S, et al; ASCEND Study Group. A phase 3 trial of pirfenidone in patients with idiopathic pulmonary fibrosis. N Engl J Med. 2014;370:2083–92.
6. Richeldi L, du Bois RM, Raghu G, et al; INPULSIS Trial Investigators. Efficacy and safety of nintedanib in idiopathic pulmonary fibrosis. N Engl J Med. 2014;370:2071–82.
7. He L, Hannon GJ. MicroRNAs: small RNAs with a big role in gene regulation. Nat Rev Genet. 2004;5:522–31.
8. Xie T, Liang J, Guo R, Liu N, Noble PW, Jiang D. Comprehensive microRNA analysis in bleomycin-induced pulmonary fibrosis identifies multiple sites of molecular regulation. Physiol Genomics. 2011;43:479–87.
9. Yamada M, Kubo H, Ota C, et al. The increase of microRNA-21 during lung fibrosis and its contribution to epithelial-mesenchymal transition in pulmonary epithelial cells. Respir Res. 2013;14:95.
10. Liu G, Friggeri A, Yang Y, et al. miR-21 mediates fibrogenic activation of pulmonary fibroblasts and lung fibrosis. J Exp Med. 2010;207:1589–97.
11. Pandit KV, Corcoran D, Yousef H, et al. Inhibition and role of let-7d in idiopathic pulmonary fibrosis. Am J Respir Crit Care Med. 2010;182:220–9.
12. Yang S, Banerjee S, de Freitas A, et al. Participation of miR-200 in pulmonary fibrosis. Am J Pathol. 2012;180:484–93.
13. Liu B, Jiang T, Hu X, et al. Downregulation of microRNA-30a in bronchoalveolar lavage fluid from idiopathic pulmonary fibrosis patients. Mol Med Rep. 2018;18:5799–806.
14. Ren L, Yang C, Dou Y, Zhan R, Sun Y, Yu Y. MiR-541-5p regulates lung fibrosis by targeting cyclic nucleotide phosphodiesterase 1A. Exp Lung Res. 2017;43:249–58.
15. Thery C, Zitvogel L, Amigorena S. Exosomes: composition, biogenesis and function. Nat Rev Immunol. 2002;2:569–79.
16. Cui H, Banerjee S, Xie N, et al. MicroRNA-27a-3p is a negative regulator of lung fibrosis by targeting myofibroblast differentiation. Am J Respir Cell Mol Biol. 2016;54:843–52.
17. Wynn TA. Cellular and molecular mechanisms of fibrosis. J Pathol. 2008;214:199–210.
18. Fernandez IE, Eickelberg O. The impact of TGF-beta on lung fibrosis: from targeting to biomarkers. Proc Am Thorac Soc. 2012;9:111–6.
19. Kang H. Role of microRNAs in TGF-beta signaling pathway-mediated pulmonary fibrosis. Int J Mol Sci. 2017;18:pii: E2527.
20. Huang C, Xiao X, Yang Y, et al. MicroRNA-101 attenuates pulmonary fibrosis by inhibiting fibroblast proliferation and activation. J Biol Chem. 2017;292:16420–39.
21. Fierro-Fernandez M, Busnadiego O, Sandoval P, et al. miR-9-5p suppresses pro-fibrogenic transformation of fibroblasts and prevents organ fibrosis by targeting NOX4 and TGFBR2. EMBO Rep. 2015;16:1358–77.
22. Stolzenburg LR, Wachtel S, Dang H, Harris A. miR-1343 attenuates pathways of fibrosis by targeting the TGF-beta receptors. Biochem J. 2016;473:245–56.
23. Zeng X, Huang C, Senavirathna L, Wang P, Liu L. miR-27b inhibits fibroblast activation via targeting TGF-beta signaling pathway. BMC Cell Biol. 2017;18:9.
24. Harrison JH Jr, Lazo JS. High dose continuous infusion of bleomycin in mice: a new model for drug-induced pulmonary fibrosis. J Pharmacol Exp Ther. 1987;243:1185–94.
25. Inomata M, Kamio K, Azuma A, et al. Pirfenidone inhibits fibrocyte accumulation in the lungs in bleomycin-induced murine pulmonary fibrosis. Respir Res. 2014;15:16.
26. Kamio K, Azuma A, Usuki J, et al. XPLN is modulated by HDAC inhibitors and negatively regulates SPARC expression by targeting mTORC2 in human lung fibroblasts. Pulm Pharmacol Ther. 2017;44:61–9.
27. Ashcroft T, Simpson JM, Timbrell V. Simple method of estimating severity of pulmonary fibrosis on a numerical scale. J Clin Pathol. 1988;41:467–70.
28. Hong Y, Cao H, Wang Q, et al. MiR-22 may suppress fibrogenesis by targeting TGFbetaR I in cardiac fibroblasts. Cell Physiol Biochem. 2016;40:1345–53.
29. Midgley AC, Rogers M, Hallett MB, et al. Transforming growth factor-beta1 (TGF-beta1)-stimulated fibroblast to myofibroblast differentiation is mediated by hyaluronan (HA)-facilitated epidermal growth factor receptor (EGFR) and CD44 co-localization in lipid rafts. J Biol Chem. 2013;288:14824–38.
30. Yang Z, Sun Z, Liu H, et al. Connective tissue growth factor stimulates the proliferation, migration and differentiation of lung fibroblasts during paraquat-induced pulmonary fibrosis. Mol Med Rep. 2015;12:1091–7.
31. Yaekashiwa M, Nakayama S, Ohnuma K, et al. Simultaneous or delayed administration of hepatocyte growth factor equally represses the fibrotic changes in murine lung injury induced by bleomycin. A morphologic study. Am J Respir Crit Care Med. 1997;156:1937–44.
32. Aono Y, Nishioka Y, Inayama M, et al. Imatinib as a novel antifibrotic agent in bleomycin-induced pulmonary fibrosis in mice. Am J Respir Crit Care Med. 2005;171:1279–85.
33. Colombo M, Raposo G, Thery C. Biogenesis, secretion, and intercellular interactions of exosomes and other extracellular vesicles. Annu Rev Cell Dev Biol. 2014;30:255–

89.
34. Andaloussi SE, Mager I, Breakefield XO, Wood MJ. Extracellular vesicles: biology and emerging therapeutic opportunities. Nat Rev Drug Discov. 2013;12:347–57.
35. Tan JL, Lau SN, Leaw B, et al. Amnion epithelial cell-derived exosomes restrict lung injury and enhance endogenous lung repair. Stem Cells Transl Med. 2018;7:180–96.
36. Martin-Medina A, Lehmann M, Burgy O, et al. Increased extracellular vesicles mediate WNT-5A signaling in idiopathic pulmonary fibrosis. Am J Respir Crit Care Med. 2018;198:1527–38.
37. Yang H, Li W, Zhang Y, et al. Regulatory role of miR-18a to CCN2 by TGF-β1 signaling pathway in pulmonary injury induced by nano-SiO_2. Environ Sci Pollut Res Int. 2018;25:867–76.
38. Chen YC, Chen BC, Yu CC, Li SH, Lin CH. miR-19a, -19b, and -26b Mediate CTGF Expression and Pulmonary Fibroblast Differentiation. J Cell Physiol. 2016;231:2236–48.
39. Singh Y, Garden OA, Lang F, Cobb BS. MicroRNA-15b/16 enhances the induction of regulatory T cells by regulating the expression of Rictor and mTOR. J Immunol. 2015;195:5667–77.
40. Inomata M, Kamio K, Azuma A, et al. Antifibrotic effect of microRNA-16 in human lung fibroblasts. Am J Respir Crit Care Med. 2018;197:A2295.

(Received, August 5, 2019)
(Accepted, October 29, 2019)
(J-STAGE Advance Publication, November 28, 2019)